*Carbohydrate Polymers* **13** (1990) 317–333

# Phase Equilibria for Xanthan Gum in Ethanol–Water Solutions

R. Gonzales, M. R. Johns,* P. F. Greenfield

Department of Chemical Engineering, The University of Queensland, St Lucia, Queensland 4067, Australia

&

G. W. Pace

Bioagrix Pty Ltd, PO Box 377, Lindfield, New South Wales 2070, Australia

(Received 4 October 1989; accepted 16 October 1989)

*ABSTRACT*

*An equilibrium phase diagram was developed for the ternary system xanthan/ethanol/water at 15°C and 1% w/v KCl. The data demonstrate that xanthan precipitation by ethanol occurs at ethanol levels of 30% w/w solvent or greater. The effect of ethanol concentration on xanthan solubility is markedly different from that of ethanol on proteins and is characterised by a sudden transition from high solubility to virtual insolubility over a narrow range (20–30% w/w solvent) of solvent-ethanol content. Further increases in ethanol content gave no improvement in xanthan yield but increasing xanthan purity.*

*The applicability of three equilibrium-solubility models commonly used to describe other polymer-solvent systems is discussed. Of these, that based on solution theory appears to be the most useful. The solubility data are used to predict how xanthan recovery from fermentation broths by ethanolic precipitation can be optimised in terms of yield.*

## INTRODUCTION

Xanthan gum, an anionic polysaccharide produced by *Xanthomonas campestris*, is typically separated from its fermentation broth by pre-

*To whom correspondence should be addressed.



*Carbohydrate Polymers* 0144-8617/90/$03.50 — 

cipitation with a suitable solvent (Gonzales *et al.*, 1989). Precipitation processes involving the use of salts, organic solvents, or synthetic polymers as precipitants are commonly described in the literature as early steps in the purification of biopolymers from such broths. The development of efficient and reliable large-scale precipitation processes depends on a knowledge of the effects of different physical and chemical factors on the precipitation. Acquiring phase-equilibria data and solubilities in multicomponent solutions for these biopolymers is essential. Such data are, however, extremely scarce (Olien, 1987).

In the absence of experimentally derived property data for many biopolymers, it would be of great value to use predictive models to design purification processes. To some extent, it might be expected that similar models would apply to a wide variety of biopolymers, since they have many properties in common. For example, xanthan, proteins, and nucleic acids are all polyelectrolytes — charged biopolymers. Xanthan, cellulose, starch, and dextrans are biopolymers possessing a glucose backbone. In a broader sense, xanthan and the synthetic polymer polystyrene, for instance, both consist of repeating subunits assembled into chains of varying length. On the other hand, even small variations in biopolymer structure confer major changes in properties, as is best evidenced by the proteins.

Currently, there appear to be three general approaches to predicting polymer solubility. The first has been widely employed for the design of processes requiring precipitation of proteins from aqueous solution by using concentrated salt solutions or organic solvents. In the former case, the logarithm of protein solubility is a linear function of the ionic strength of the solution and is affected by temperature, pH, and the type of salt (Green & Hughes, 1955). This plot is commonly called a Cohn plot (Foster *et al.*, 1971). The application of theoretical models to the salting out of proteins has been summarised recently by Przybycien and Bailey (1989). In the latter instance, a similar plot of protein solubility against solvent dielectric constant can be used for process design according to eqn (1):

$$\log S = \frac{k}{D_s^2} + \log S_0 \tag{1}$$

where $S$ is the protein solubility ($S_0$ is the initial protein solubility); $D_S$ is the solvent dielectric constant, and $k$ is a constant. The dielectric constant is a measure of the ability of a solvent to increase the attractive forces between solute molecules, which eventually brings about precipitation.

A second approach uses the Brönsted partition equation (Albertsson, 1971):

$$\frac{C_1}{C_2} = e^{\lambda M/TK} \tag{2}$$

where $C_1$, $C_2$ are solute concentrations in phases 1 and 2, respectively; $M$ is the polymer molecular weight; $T$ is the absolute temperature; $K$ is the Boltzmann constant; and $\lambda$ is an energetic parameter based on the solvent/polymer interactions. This model has been successfully used to describe the partitioning of proteins and nucleic acids according to molecular weight (Albertsson, 1971) and in the fractionation of dextran by using ethanol (Barker *et al.*, 1987).

A third, more rigorous approach is to apply a modified solution theory to characterise the phase equilibria of synthetic-polymer solutions (Tompa, 1956). In general, a system containing a polydisperse polymer, in either a single solvent or a mixture of solvents, is said to be in equilibrium when the different phases have the same chemical potential. The phase diagram for a solution of $n+1$ components, for instance, made up of a solvent and $n$ polymer components (each length of polymer being treated as one component), is a diagram within an $n$-dimensional polyhedron in $n$-dimensional space. For a monodisperse polymer in solution with a solvent and nonsolvent (e.g. water and ethanol), the diagram will therefore be a regular triangular phase-equilibrium diagram.

Phases in equilibrium lie on an $(n-1)$-dimensional binodial surface. On a triangular chart, this is also called the *phase envelope*. The binodial is the limit of absolute stability of the homogeneous phases (Tompa, 1956). Another curve, called the *spinodial*, divides the stable and metastable regions from the absolutely unstable ones. In thermodynamic terms, the binodial is the locus of points described by the following condition:

$$\Delta\mu_1' = \Delta\mu_1''; \Delta\mu_2' = \Delta\mu_2''; \Delta\mu_a' = \Delta\mu_a'' \tag{3}$$

while the spinodial is the curve that satisfies the equation:

$$\left[\frac{\partial x_3}{\partial x_2}\right] G_2 = \left[\frac{\partial x_3}{\partial x_2}\right] G_3 \tag{4}$$

where $\Delta\mu_1'$ is the change in chemical potential of component 1 in one phase, and so on; and $x_2$ and $x_3$ are the mole fractions of components 2

and 3, respectively. The parameter $G_2$ is defined as:

$$G_2 = \frac{\partial(\Delta G)}{\partial x_2} \tag{5}$$

The occurrence of spinodials is characteristic of polymer/solvent/nonsolvent systems (Tompa, 1956).

The behaviour of ternary systems of polymer/solvent/nonsolvent with different properties has been predicted by Tompa (1956), using the Flory–Huggins theory. As the interaction constant, $\chi$, increases, the two-phase region is shown to occupy an increasing portion of the triangular chart, $\chi$ being a measure of the affinity of the polymer to the solvents. For systems in which the molar volume of the polymer is very large compared with the molar volume of the solvent and $\chi$ is between 1 and 2, Tompa (1956) predicted the phase diagram to be as shown in Fig. 1. In such systems, one phase contains a large amount of polymer and varying amounts of solvent and nonsolvent, whereas the other phase is essentially pure liquid.

The application of solution theory to predict the behaviour of biopolymers is confronted by two problems. First, the theory has been developed for molecules that are polydisperse with respect to size only. This assumes that the monomer, or repeating unit of the polymer chain,

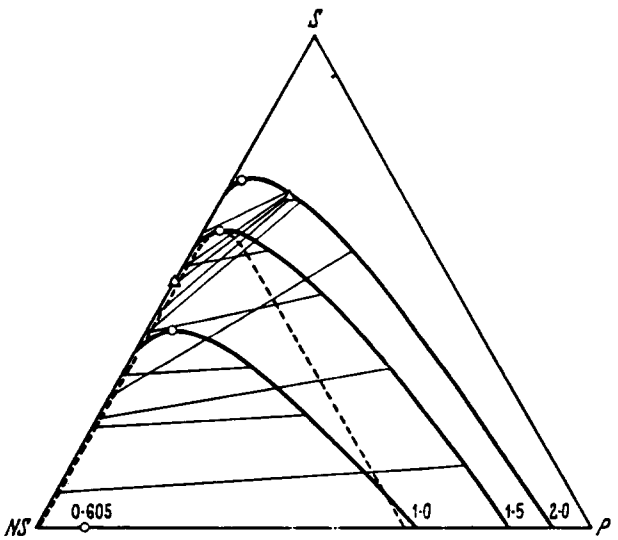


**Fig. 1.** Phase diagrams predicted for a system of polymer/nonsolvent/solvent with molar-volume ratio of 100 and $\chi$ values between 1 and 2. Spinodial shown (– – –) is for $\chi = 1{\cdot}5$ (Tompa, 1956).

has the same structure throughout, with variations occurring with respect to chain length only. Biopolymers, such as xanthan, can be polydisperse with respect to both size and molecular structure, that is, within a single xanthan chain, branching may be irregular, and the structure of the branches may differ in acetate and pyruvate substitution. The latter has been demonstrated to affect xanthan precipitation in ethanolic solution (Sandford *et al.*, 1978). A second limitation is the presence of higher-ordered structures of biopolymer in solution at concentrations that are dilute with respect to those found with synthetic polymers. Nevertheless, the theory of polymer solutions and polymer fractionation as developed for synthetic polymers may be useful in predicting and rationalising the behaviour of xanthan, although its application may not be rigorously correct in every aspect.

The work described in this paper investigated the solubility of xanthan in aqueous solutions of ethanol so as to develop phase-equilibrium data. These were then analysed according to the three approaches described above to evaluate their usefulness for the design of a xanthan-precipitation process.

## MATERIALS AND METHODS

### Preparation of stock solutions

Stock solutions containing from 0·5 to 2% (w/w) xanthan (Food grade, Jungbunzlauer) were made by methods described by Jeanes *et al.* (1961). Stock solutions of KCl (Ajax Chemicals, Sydney, Australia) contained 23% (w/w) KCl. Sodium chloride stock solution, used for the determination of the molecular weight of xanthan, was made by passing a 15% (w/v) solution through a 0·45-$\mu$m Millipore filter. Absolute ethanol (May & Baker, Melbourne, Australia) was AR Grade.

### Preparation of mixtures

Duplicate mixtures consisting of known weights of xanthan and KCl stock solutions were made in preweighed 250-ml centrifuge bottles to give a total final mass of 200 g of salt-free mixture including ethanol. Distilled water was added as required. The centrifuge bottles were placed in an orbital shaker controlled at 15 ± 0·25°C and shaken at 120 opm for at least 36 h before adding the required amount of ethanol. After mixing for a further 24 h, the precipitate was recovered by centrifugation at 14 000 *g* for 30 min.

## Analyses

To determine xanthan concentration, the precipitate and a sample of the supernatant were dialysed against running tap water for 24 h and then against distilled water for a minimum of 72 h by using cellulose membranes (Union Carbide, Chicago, USA) with a 6000–8000-molecular-weight cut-off. The dialysate was dried at 110°C to a constant weight.

Ethanol analysis was performed by using a Varian 3700 gas chromatograph (Varian Techtron Pty Ltd, Springvale, Australia) with FID detection at 210°C. An aliquot of supernatant solution was diluted with distilled water to contain less than 10% (w/w) ethanol, and 5 ml were then mixed with 10% isopropanol (5 ml) as internal standard and diluted to 50 ml with water. From this solution, 10 $\mu$l were injected at 150°C onto a 2-m × 3-mm glass column containing 3% Carbowax 1500 on Graphpak GC at 90°C. An SIC recording integrator was used for area measurement.

The potassium concentration of the supernatant was determined by atomic-absorption spectrophotometry (Varian AA775, Varian Techtron Pty Ltd, Springvale, Australia) with flame emission (766·5 nm) by using a neutral air–acetylene flame. Caesium, as $CeCl_2$, was added to the sample (1000 ppm) as an ionisation suppressant. Chloride concentration was determined by suppressed-ion chromatography by using a Dionex Ion Chromatograph (2010i) equipped with HPIC AS4 Anion column, AG4 Guard column, and an anion fibre suppressor (Dionex Corp, USA). Detection was achieved by using a Dionex conductivity detector with a temperature coefficient of 1·7. An injection volume of 50 $\mu$l was used. The mobile phase consisted of 0·0028 M $NaHCO_3$ and 0·0022 M $NaCO_3$ with 0·025 N $H_2SO_4$ as regenerant at a flow rate of 2 ml/min.

## Molecular-weight determination

The average molecular weight of xanthan was measured by using viscometric methods. To an aliquot of xanthan stock solution of supernatant containing 0·06–0·07 g xanthan, NaCl stock solution was added to 10% (w/v) and the solution held at room temperature for at least 24 h for uniform hydration. The xanthan was precipitated with ethanol (100 ml), collected by centrifuging at 14 000 *g* for 30 min, and washed with ethanol–water mixtures (50%–100% ethanol (v/v soln)) until no chloride was detected in the wash liquid on treatment with silver nitrate. The xanthan was dried *in vacuo* at room temperature and weighed.

A solution of 0·06% (w/v) purified xanthan in 0·1 M NaCl was held at room temperature until it had a visibly uniform consistency. It was then stirred (100 rpm) for at least 12 h to reduce microgel size and aggregation. From this, solutions were made with concentrations ranging from 0·01 to 0·05% (w/v) in 0·1 M NaCl and filtered through a 0·45-$\mu$m Millipore filter. Their viscosity was measured at shear rates in the range 24·1–3650 $s^{-1}$ by using a Contraves Rheomat 115 viscometer.

## RESULTS AND DISCUSSION

### Equilibrium solubility of xanthan

Experiments were conducted to measure the equilibrium solubility of xanthan in aqueous ethanol at 15°C. Where phase separation occurred, the compositions of the resulting phases were analysed and the results checked by mass-balance calculation. These data are presented in Table 1, on a salt-free basis, and used to generate a ternary-phase diagram on enlarged right triangular co-ordinates (Fig. 2(a)). A binodial curve was drawn through these data, and the corresponding ethanol-distribution curve is plotted in Fig. 2(b). These data are the first reported for xanthan, if not for the solubility of any polysaccharide, in solvent mixtures.

**TABLE 1**
Composition of Initial Xanthan Solutions and Phases at Equilibrium

| *Bulk mixtures* | | *Precipitate* | | *Supernatant* | |
|---|---|---|---|---|---|
| *Ethanol* | *Xanthan* | *Ethanol* | *Xanthan* | *Ethanol* | *Xanthan* |
| 0·2385 | 0·00697 | 0·11 | 0·0093 | 0·249 | 0·0067 |
| 0·27690 | 0·00710 | 0·16 | 0·0082 | 0·289 | 0·00621 |
| 0·2790 | 0·00899 | 0·19 | 0·0105 | 0·290 | 0·00833 |
| 0·2994 | 0·00701 | 0·217 | 0·01252 | 0·390 | 0·0003 |
| 0·2997 | 0·00601 | 0·21 | 0·0099 | 0·309 | 0·00549 |
| 0·2998 | 0·00701 | 0·249 | 0·0123 | 0·354 | 0·0004 |
| 0·3997 | 0·00500 | 0·28 | 0·0162 | 0·451 | 0·0001 |
| 0·3999 | 0·00500 | 0·23 | 0·0132 | 0·49 | 0·0001 |
| 0·5989 | 0·00301 | 0·39 | 0·0226 | 0·63 | 0·00012 |
| 0·5992 | 0·00301 | 0·50 | 0·0299 | 0·61 | 0·0001 |
| 0·89615 | 0·00211 | 0·90 | 0·0432 | 0·896 | 0·00010 |
| 0·89722 | 0·00206 | 0·80 | 0·0399 | 0·900 | 0·00005 |

All data are presented as mass fractions.

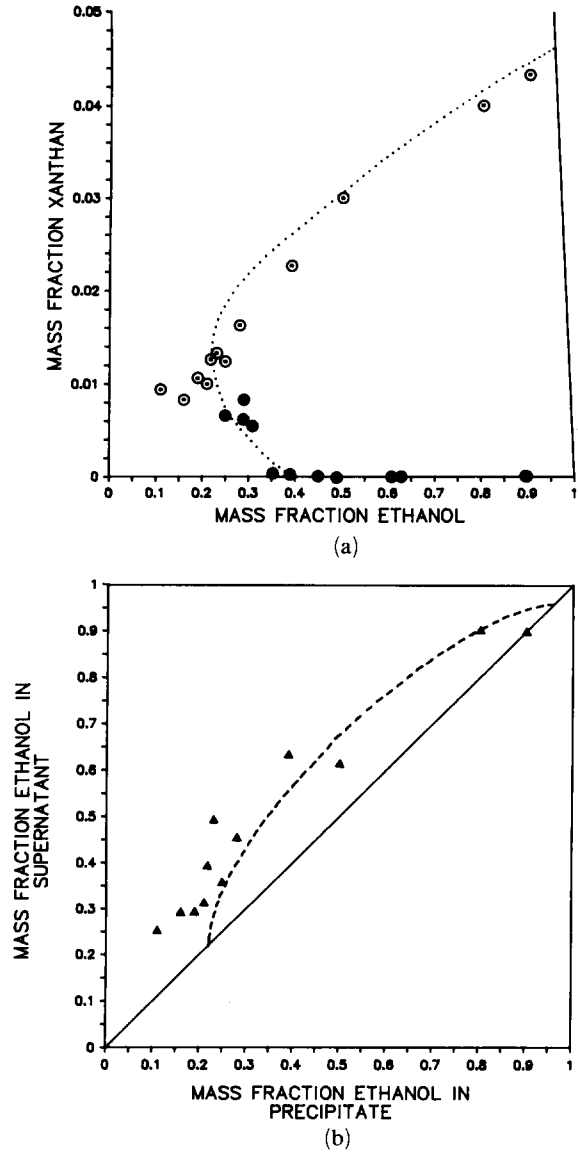


**Fig. 2.** (a) A binodial curve (...) traced through points representing the composition of precipitates and supernatants of the separating mixtures: (⊙) precipitate; (●) supernatant. (b) The corresponding ethanol-distribution curve (– – –) showing the location of experimental values (▲). Both curves are within the error limits of the points that are seen in Fig. 3.

Xanthan solubility in aqueous ethanol is greatly affected by the ethanol content of the solvent. In solvent containing less than 20% (w/w) ethanol, xanthan solubility is limited only by the formation of weak-gel structures at high xanthan concentrations. Saturation occurring at lower xanthan concentrations in these solvent mixtures is difficult to detect by conventional methods (e.g. turbidometric, refractive-index measurements) because the solutions are not optically clear.

As the ethanol concentration in the solvent increases from 20 to 40% (w/w), xanthan solubility decreases rapidly, and, above this range, xanthan is insoluble. Xanthan precipitate from bulk solutions of these compositions appears gel-like and swollen. This may be due to the high xanthan concentration, which causes the formation of entanglement networks or weak-gel mixtures (Morris *et al.*, 1983; Clark & Ross-Murphy, 1987). Sandford *et al.* (1977) reported that the nature of the xanthan precipitate from ethanolic solutions varied according to the thermal history and pyruvate content of the xanthan. Xanthan high in pyruvate (>4%) formed a cohesive stringy precipitate, whereas low-pyruvate xanthan (2·5–3·5%) was a less cohesive, particulate material. Brief heating of low-pyruvate xanthan solutions (e.g. 3 min at 95°C) led to a precipitate similar to that of high-pyruvate xanthan.

**Application of solubility models**

The binodial curve in Fig. 2(a) shows great similarity with the curves predicted by Tompa (1956) for large synthetic polymers, for which values of the interaction constant fall between 1 and 2 (Fig. 1). Properties predicted for these polymers can also explain those observed for the xanthan/ethanol/water system. For instance, xanthan mixtures having identical compositions separated into phases of different compositions at equilibrium, as seen in Fig. 3(a). This would seem to indicate the existence of metastable regions, commonly represented by a spinodial curve. The existence of a heterogeneous double-plait point, arising when another binodial develops around a point of the spinodial, has also been predicted for systems containing large polymers (Tompa, 1956). The presence of such a feature in the xanthan/ethanol/water system is indicated by the abrupt shift in the slopes of the actual tie-lines of the mixtures, shown in Fig. 3(b), between 0·10 and 0·25 mass fraction ethanol. The models of Tompa therefore appear applicable to a description of the solubility of at least some biological polymers in mixtures of solvent and nonsolvent.

To ascertain the usefulness of Cohn plots for predicting the behaviour of xanthan in aqueous ethanol solutions, xanthan solubility at equilibrium was plotted against solvent composition (Fig. 4) and the cor-

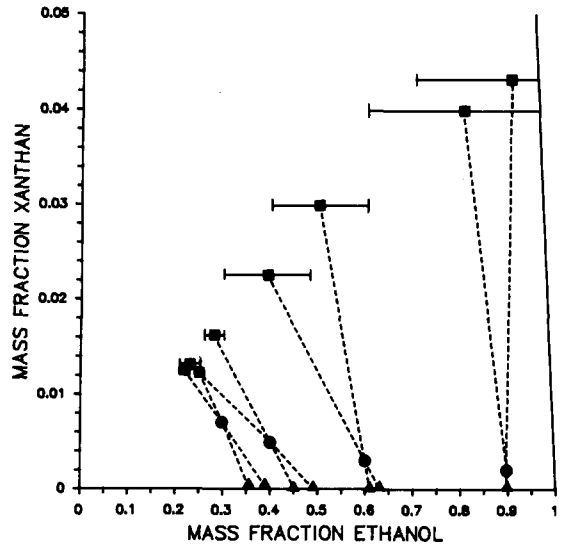


(a)

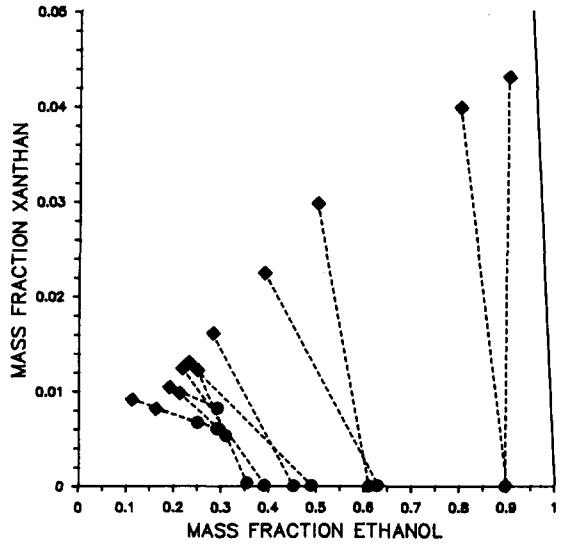


(b)

**Fig. 3.** (a) Evidence of a metastable region: separation of identical bulk mixtures of xanthan/water/ethanol at 15°C into phases of different composition. Error bars represent 95% confidence limits. Errors for the xanthan mass fraction are very small compared with errors for the ethanol mass fraction: (●) bulk mixture; (■) precipitate; (▲) supernatant. (b) Evidence of a double-plait point in the xanthan/ethanol/water system. Actual tie-lines are drawn between the precipitate and supernatant points of the mixtures considered in Fig. 2: (●) precipitate; (◆) supernatant.

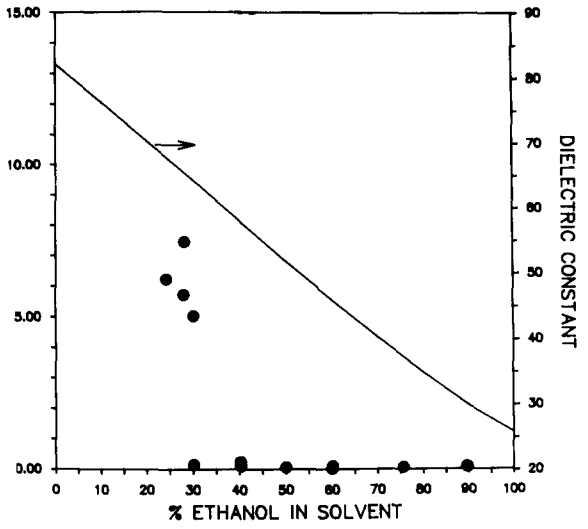


**Fig. 4.** Solubility of xanthan in ethanol–water mixtures at 15°C, showing the variation of the dielectric constant with solvent composition: (●) solubility of xanthan; (——) dielectric constant.

responding dielectric-constant values, calculated from the data reported by Akerlöf (1932) for ethanol–water mixtures. The plot demonstrates that the effect of ethanol in reducing xanthan solubility occurs over a very narrow range. There appears to be a critical dielectric-constant value ($\approx 65$) at which this transition occurs. To our knowledge, there is no mention of a critical dielectric-constant value reported for proteins or other biopolymers. Depression of protein solubility with ethanol content occurs more gradually, as the data of Chan *et al.* (1986) for the ethanolic precipitation of soya protein demonstrate. The rapid decrease in solubility with solvent composition suggests that Cohn-like equations are of little benefit for predicting xanthan solubility, in contrast to protein precipitation.

The Brönsted equation has been used to predict the fractionation of dextran with ethanol (Barker *et al.*, 1987). To determine whether selective precipitation of xanthan on the basis of molecular size had occurred, the intrinsic viscosity $[\eta]$ of the supernatants of xanthan solutions containing lower quantities of ethanol ($\approx 30\%$ w/w) was calculated and compared with that of the parent xanthan. The intrinsic viscosity can be related to the weight-average molecular weight, $M_w$, of polymers by use of the Mark–Houwink equation:

$$[\eta] = K M_w^a \tag{6}$$

Milas *et al.* (1985) reported the Mark–Houwink constants for xanthan in 0·1 M NaCl to be $1{\cdot}7 \times 10^{-4}$ and 1·14 for $K$ and $a$, respectively. These values are applicable only when the intrinsic viscosity at zero shear rate is used. In this study, this value was calculated by using the Huggins equation and extrapolating the intrinsic-viscosity values obtained to zero shear rate.

The results demonstrated that the molecular weights of xanthan in the supernatants treated with ethanol were similar to those of the parent xanthan ($2 \times 10^6$ daltons), suggesting that higher-molecular-weight xanthan was not precipitated preferentially to smaller molecules. The Brönsted equation appears of limited utility in this instance.

Unlike dextran, it is likely that fractional precipitation of xanthan is more complex. Innate properties of xanthan such as subunit structure, the degree of polymerisation, solution conformation, and other factors known to affect fractionation efficiency may prevent xanthan from fractionating in ethanol (Mencer, 1988). The influence of structure on xanthan precipitation was demonstrated by Sandford *et al.* (1978), who achieved the fractionation of xanthan on the basis of pyruvate content by using ethanol. Other methods of fractionation, such as fractional dissolution, salting out, or using a different nonsolvent, may work better for the system. But the effectiveness of these methods can be limited by the solution conformation of xanthan, which restricts the concentration range where the method is applicable. Some authors have used gel-filtration columns to separate the various fractions obtained from sonication of native xanthan (Lecourtier & Chauveteau, 1984; Sato *et al.*, 1984; Stokke *et al.*, 1986).

## Optimal conditions for xanthan recovery

Although the solution-theory approach appears to show most promise for predicting the solubility of xanthan in water–ethanol solutions, the actual data shown in Fig. 2 can be used very effectively to design a separation process.

The equilibrium-solubility data permit optimal conditions for xanthan recovery to be predicted. Figure 5(a) shows the relationship between xanthan recovery and ethanol concentration in the solvent. Clearly, to maximise recovery of the polysaccharide, the solvent should contain more than 30% (w/w) ethanol. Furthermore, a solvent with a higher ethanol content will not increase xanthan recovery to an extent that will justify the additional ethanol added.

The purity of the precipitate is important to final-product quality. It is useful to know the effect of solvent composition on the retention of

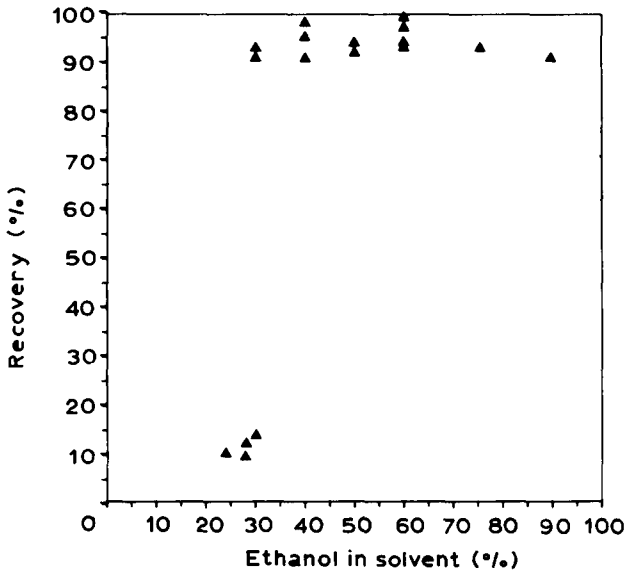


(a)

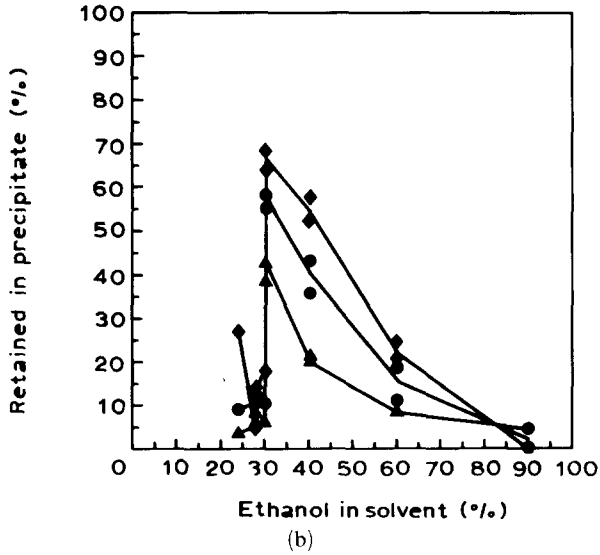


(b)

**Fig. 5.** (a) Recovery of xanthan with varying ethanol content in the solvent. Recovery is defined as the ratio of the amount of xanthan in the precipitate to the amount of xanthan originally in solution; (b) effect of solvent composition on precipitate purity. Retention in the precipitate is calculated as the ratio of the weight of the component in the precipitate to that weight originally in solution: (◆) potassium chloride; (●) water; (▲) ethanol.

impurities, such as salt, ethanol, and water, in the precipitated xanthan. Figure 5(b) shows the retention of these components in crude xanthan precipitated with solvents of varying composition. Whereas increasing the ethanol content of the solvent above 30% (w/w) does not increase xanthan recovery, it achieves an increasing degree of product purity. The increase in purity achieved with respect to water and potassium chloride was larger than might be expected from dilution by ethanol alone, especially as the ethanol content of the solvent increased. This may have been due to the nature of the precipitate. At high ethanol levels, the precipitated xanthan was observed to be more compact, and presumably the amount of interstitial water, containing potassium chloride, is reduced. This explanation is supported by the approximately parallel relationship between the curves representing the two impurities in Fig. 5(b).

Conversely, potassium chloride has poor solubility in ethanol and it might be expected that, at high ethanol concentrations in the solvent, the salt content of the xanthan precipitate would increase owing to co-precipitation of potassium chloride. There is, however, no evidence of this occurring.

The ethanol content of the precipitate also fell with increasing ethanol content in the solvent and was lower than expected. This again was probably the result of the increasing compactness of the precipitate.

A fermentation broth will contain other impurities, including carbohydrates, proteins, and complex organic compounds, that will be retained in the crude precipitate. The removal of these substances is essential if the final product is to be used for food applications. If retention of these other impurities follows the trend observed in Fig. 5(b), then the addition of large amounts of ethanol would maximise purity of the product at the price of increased distillation costs for solvent reuse. Alternatively, minimising the amount of ethanol used would increase post-precipitation purification costs. This is the best strategy where low purity is not a concern. Optimizing solvent use therefore requires balancing the costs of recovering the solvent for reuse and the costs of further production purification.

A number of parameters can be made the subject of optimisation studies to increase the efficiency of xanthan recovery with ethanol. The previously developed phase diagram permits the prediction of the best conditions without resorting to extensive experimentation. For example, the benefits of recovering xanthan from a more concentrated fermentation broth can be assessed. Currently, xanthan fermentations can produce broths containing up to 3% (w/w) xanthan (Ellwood *et al.*, 1986). Dilution of the broth is usually unavoidable in downstream processing, but high dilution is clearly undesirable since it increases the

volume of fluid to be processed. This reduces productivity and increases processing costs significantly.

Consider the two feeds $F_1$ and $F_2$ in Fig. 6, where $F_1$ contains half the xanthan content of $F_2$. The addition of ethanol to the feeds yields bulk

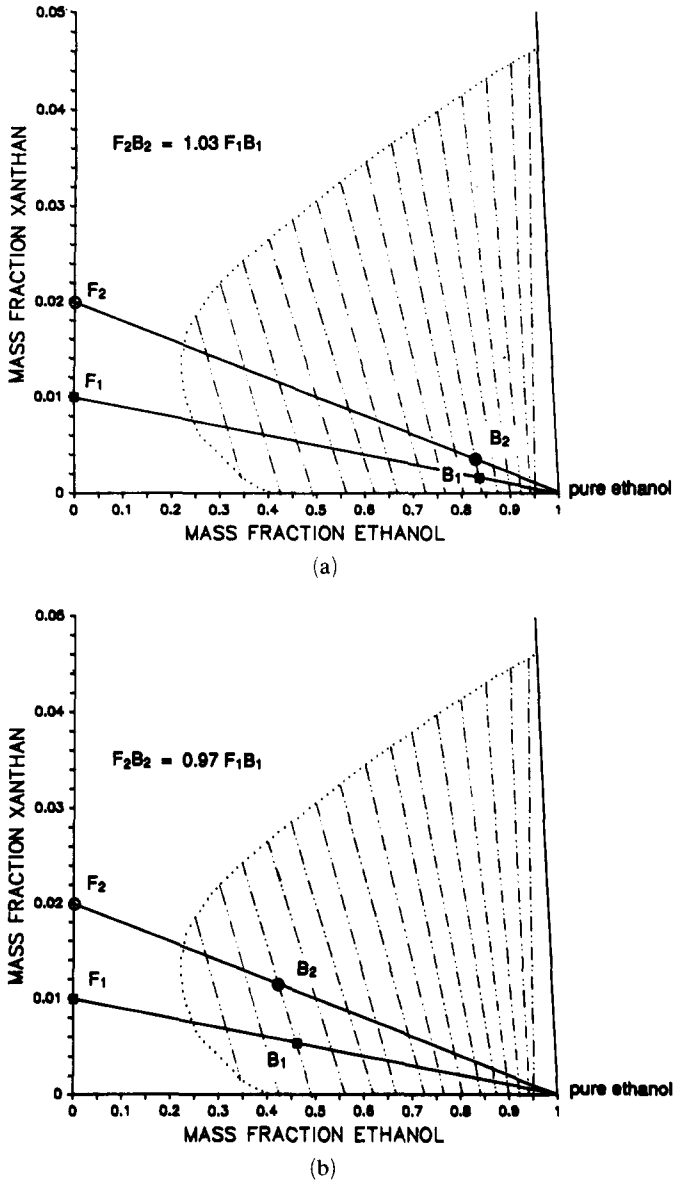


**Fig. 6.** Optimisation of ethanol use in xanthan precipitation: (a) xanthan concentration in the feed; (b) reduction of amount of ethanol used. The dashed lines (— ··· —) represent tie-lines.

mixtures $B_1$ and $B_2$, respectively. From the inverse-lever-arm rule (Perry & Green, 1984), the amount of ethanol added to $F_1$ and $F_2$ will be proportional to the lengths of the line segments $F_1B_1$ and $F_2B_2$, respectively. If the final condition of the precipitate is fixed, then the tie-line containing that precipitate composition will also fix the final composition of the bulk mixture.

The tie-lines in the high-ethanol region are very steep. If $B_1$ and $B_2$ lie in this region, there is very little difference in the length of line segments $F_1B_2$ and $F_2B_2$. In Fig. 6(a), for example, the length of $F_2B_2$ is only 1·03 times the length of $F_1B_1$. Thus, the phase diagram predicts that, for the same mass of feed, doubling the xanthan concentration in the feed gives almost double the xanthan yield for the same quantity of ethanol used. If a smaller amount of ethanol is used, as in Fig. 6(b), the result is even better, for the more concentrated feed will actually use up a lower amount of ethanol to bring it to precipitation point. In using the predictive power of the phase diagram, other factors, such as the retention of impurities, the costs of distillation for solvent reuse, and costs for further purification of the crude precipitate, should not be forgotten.

## CONCLUSIONS

The precipitation of xanthan gum from aqueous solution by using ethanol is achieved above ethanol concentrations in the solvent of 30% (w/w). Unlike proteins, the yield of xanthan is not increased with the ethanol content of the solvent. In contrast, the purity of the precipitate demonstrated a marked improvement as the solution was enriched in ethanol.

Three approaches to modelling the precipitation of polymers were assessed by using the solubility data developed for the xanthan/ethanol/water system. The use of solution theory extended to synthetic-polymer solutions was found to describe the xanthan system best. More information concerning interaction constants for xanthan are needed to test the application of this theory to the design of xanthan precipitation.

## ACKNOWLEDGEMENT

The authors thank Mr K. Dobson and Mr P. Abeydeera for their expert technical assistance.

## REFERENCES

Akerlöf, G. (1932). *J. Amer. Chem. Soc.*, **54**, 4125–39.
Albertsson, P. A. (1971). *Partition of Cell Particles and Macromolecules*, 2nd edn, Wiley-Interscience, New York.
Barker, P. E., Bhambra, K. S., Alsop, R. M. & Gibbs, R. (1987). *Chem. Engng Res. Des.*, **65**, 390–5.
Chan, M. Y. Y., Hoare, M. & Dunnill, P. (1986). *Biotechnol. Bioengng*, **28**, 387–93.
Clark, A. H. & Ross-Murphy, S. B. (1987). *Adv. Polym. Sci.*, **83**, 57–197.
Ellwood, D. C., Evans, C. G. T. & Yeo, R. G. (1986). Polysaccharide. Patent No. WO 86/1830 A1.
Foster, P. R., Dunnill, P. & Lilly, M. D. (1971). *Biotechnol. Bioengng*, **8**, 713–18.
Green, A. A. & Hughes, W. L. (1955). In *Methods in Enzymology*, Vol. I, ed. S. P. Colowich & N. O. Kaplan, Academic Press, New York, p. 67.
Gonzales, R., Johns, M. R., Greenfield, P. F. & Pace, G. W. (1989). *Process Biochem.*, **24**, 200–3.
Jeanes, A., Pittsley, J. E. & Senti, F. R. (1961). *J. Appl. Polym. Sci.*, **5**, 519–26.
Lecourtier, J. & Chauveteau, G. (1984). *Macromolecules*, **17**, 1340–3.
Mencer, H. J. (1988). *Polym. Bull*, **12**, 497–505.
Milas, M., Rinaudo, M. & Tinland, B. (1985). *Polym. Bull*, **14**, 157–64.
Morris, V. J., Franklin, D. & I'Anson, K. (1983). *Carbohydr. Res.*, **121**, 13–30.
Olien, N. A. (1987). *Chem. Engng Prog.*, Oct., 45–8.
Perry, R. H. & Green, D. (ed.) (1984). *Chemical Engineers' Handbook*, 6th edn, McGraw-Hill Book Co., Singapore.
Przybycien, T. M. & Bailey, J. E. (1989). *Enzyme Microb. Technol.*, **11**, 264–76.
Sandford, P. A., Pittsley, J. E., Knutson, C. A., Watson, P. R., Cadmus, M. C. & Jeanes, A. (1977). In *Extracellular Microbial Polysaccharides*, ed. P. A. Sandford & A. Laskin, American Chemical Society, Washington, p. 193.
Sandford, P. A., Watson, P. R. & Knutson, C. A. (1978). *Carbohydr. Res.*, **63**, 253–6.
Sato, T., Norisuye, T. & Fujita, H. (1984). *Polym. J.*, **16**, 341–50.
Stokke, B. T., Elgsaeter, A. & Smidsrød, O. (1986). *Int. J. Biol. Macromol.*, **8**, 217–25.
Tompa, H. (1956). *Polymer Solutions*, Butterworths, London.